

# A Self-Promotion Mechanism for Efficient Dehydrogenation of Ethanol Catalyzed by Pincer Ruthenium and Iron Complexes: Aliphatic versus Aromatic Ligands

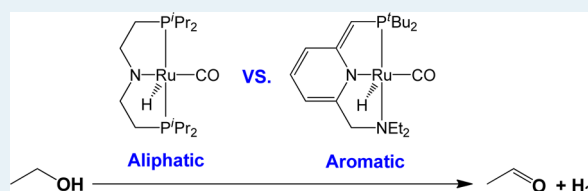
Xinzheng Yang\*

Beijing National Laboratory for Molecular Sciences, State Key Laboratory for Structural Chemistry of Unstable and Stable Species, Institute of Chemistry, Chinese Academy of Sciences, Beijing 100190, P. R. China

## Supporting Information

**ABSTRACT:** A density functional theory study reveals that the dehydrogenation of ethanol catalyzed by an aliphatic PNP pincer ruthenium complex, (PNP)Ru(H)CO ( $\mathbf{1}_{Ru}$ , PNP = bis[2-(diisopropylphosphino)ethyl]amino), proceeds via a self-promoted mechanism that features an ethanol molecule acting as a bridge to assist the transfer of a proton from ligand nitrogen to the metal center for the formation of H<sub>2</sub>. The very different catalytic properties between the aromatic and aliphatic pincer ligand in ruthenium complexes are analyzed. The potential of an iron analogue of  $\mathbf{1}_{Ru}$  (PNP)Fe(H)CO ( $\mathbf{1}_{Fe}$ ), as a catalyst for the dehydrogenation of ethanol was evaluated computationally. The calculated total free energy barrier of ethanol dehydrogenation catalyzed by  $\mathbf{1}_{Fe}$  is only 22.1 kcal/mol, which is even 0.7 kcal/mol lower than the calculated total free energy barrier of the reaction catalyzed by  $\mathbf{1}_{Ru}$ . Therefore, the potential of  $\mathbf{1}_{Fe}$  as a low-cost and high-efficiency catalyst for the production of hydrogen from ethanol is promising.

**KEYWORDS:** reaction mechanism, dehydrogenation, ethanol, ruthenium, iron, pincer ligand



With the concern of a potential energy crisis in the near future and the unwanted environmental consequences of fossil fuel consumption, people have devoted much attention in developing an environmentally friendly and unlimited energy system from renewable resources. In this respect, the idea of a “hydrogen economy”, in which hydrogen acts as an efficient, clean, and renewable energy carrier, emerged in the early 1970s.<sup>1</sup> However, low-cost, high-efficiency, and sustainable hydrogen production under ambient conditions is still one of the primary bottlenecks in the development of a hydrogen economy. Therefore, catalytic dehydrogenation of bioalcohols, such as methanol and ethanol, has attracted an increasing amount of attention in recent years because it provides a potential solution for low-cost and sustainable solar–hydrogen energy conversion.<sup>2</sup>

Although significant progress in homogeneously catalytic dehydrogenation of alcohols has been achieved,<sup>3</sup> only a few examples of dehydrogenation of aliphatic primary alcohols have been reported.<sup>4</sup> One of the most recent advances in this area is an efficient acceptorless dehydrogenation of alcohols reported by Beller and co-workers.<sup>5,6</sup> They have achieved turnover frequencies (TOFs) of 8382 and 1483 h<sup>-1</sup> (2 h) for dehydrogenations of isopropyl alcohol and ethanol, respectively, using an aliphatic PNP pincer ruthenium complex (HPNP)Ru(H)<sub>2</sub>CO {HPNP = bis[2-(diisopropylphosphino)ethyl]amine} as the catalyst under mild conditions.<sup>5</sup> The TOF for the production of ethyl acetate via the acceptorless dehydrogenation of ethanol catalyzed by (PNP)Ru(H)CO ( $\mathbf{1}_{Ru}$ ) is 1134 h<sup>-1</sup>.<sup>6</sup> Beller and co-workers also examined the catalytic property of Milstein’s aromatic pincer ruthenium

complex, (PNN)Ru(H)CO [ $\mathbf{1}_{Ru-Ar}$ , PNN = 2-(di-tert-butylphosphinomethyl)-6-(diethylaminomethyl)pyridine], for the dehydrogenation of ethanol. In contrast with  $\mathbf{1}_{Ru}$ ,  $\mathbf{1}_{Ru-Ar}$  has almost no activity under the same reaction conditions. Almost at the same time, Gusev and co-workers reported a series of ruthenium and osmium catalysts with similar aliphatic or aromatic–aliphatic pincer ligands for acceptorless dehydrogenation of alcohols.<sup>7</sup>

Although ruthenium and osmium complexes have achieved decent efficiencies in the production of hydrogen from alcohols, a major obstacle for the large-scale practical application of reported catalysts is the scarcity of the noble metals employed. The development of low-cost and environmentally benign base metal catalysts for sustainable hydrogen production remains highly attractive and challenging.<sup>8</sup> A deep understanding of the mechanistic insights of the reactions would greatly benefit the design of new catalysts.

With respect to the mechanism of catalytic dehydrogenation of alcohols, Beller and co-workers proposed a simple catalytic cycle, which contains only  $\mathbf{1}_{Ru}$  and (HPNP)Ru(H)<sub>2</sub>CO, to explain the observed reactions.<sup>5</sup> No detailed mechanistic study of the dehydrogenation of ethanol catalyzed by  $\mathbf{1}_{Ru}$  has been reported. The structures of key intermediates and rate-determining transition states in this catalytic reaction are still

Received: September 29, 2013

Revised: October 19, 2013

Published: October 21, 2013

missing. The origin of different catalytic activities of the aliphatic and aromatic pincer ligands remains unknown.

In this Letter, we report a density functional theory (DFT) study of the dehydrogenation of ethanol catalyzed by  $\mathbf{I}_{\text{Ru}}$ . A reaction mechanism with detailed free energy profiles is proposed on the basis of our calculated results. Inspired by the structures of recently reported iron and nickel complexes with aromatic and aliphatic PNP pincer ligands for catalytic hydrogenation of  $\text{CO}_2$ ,<sup>9</sup> ketones,<sup>10</sup> and alkenes,<sup>11</sup> we also explored the potential of an aliphatic PNP iron pincer complex  $\mathbf{I}_{\text{Fe}}$ , which was constructed computationally by replacing the ruthenium atom in  $\mathbf{I}_{\text{Ru}}$  with an iron atom, as a catalyst for dehydrogenation of ethanol. In addition, the low catalytic activity of  $\mathbf{I}_{\text{Ru-Ar}}$  for dehydrogenation of ethanol is also analyzed on the basis of DFT calculations.

All DFT calculations in this study were performed using the Gaussian 09 suite of *ab initio* programs<sup>12</sup> for the M06<sup>13</sup> functional with the 6-31++G(d,p) basis set for H, C, N, O, and P,<sup>14</sup> and the Stuttgart relativistic effective core potential basis set for Ru (ECP28MWB) and Fe (ECP10MDF).<sup>15</sup> Other computational details are provided in the Supporting Information. Unless otherwise noted, the energies reported in this paper are Gibbs free energies with solvent effect corrections for ethanol.

Although detailed energy barriers of the dehydrogenation of ethanol catalyzed by  $\mathbf{I}_{\text{Ru}}$  and  $\mathbf{I}_{\text{Fe}}$  are slightly different, calculated results indicate that these catalytic reactions follow similar reaction pathways. Therefore, the reaction mechanisms for the dehydrogenation of ethanol catalyzed by  $\mathbf{I}_{\text{Ru}}$  and  $\mathbf{I}_{\text{Fe}}$  are shown in one scheme (Scheme 1). Panels a and b of Figure 1 show the calculated free energy profiles of the reaction catalyzed by  $\mathbf{I}_{\text{Ru}}$

and  $\mathbf{I}_{\text{Fe}}$ , respectively. Figure 2 shows the optimized structures of key transition states in the reaction.

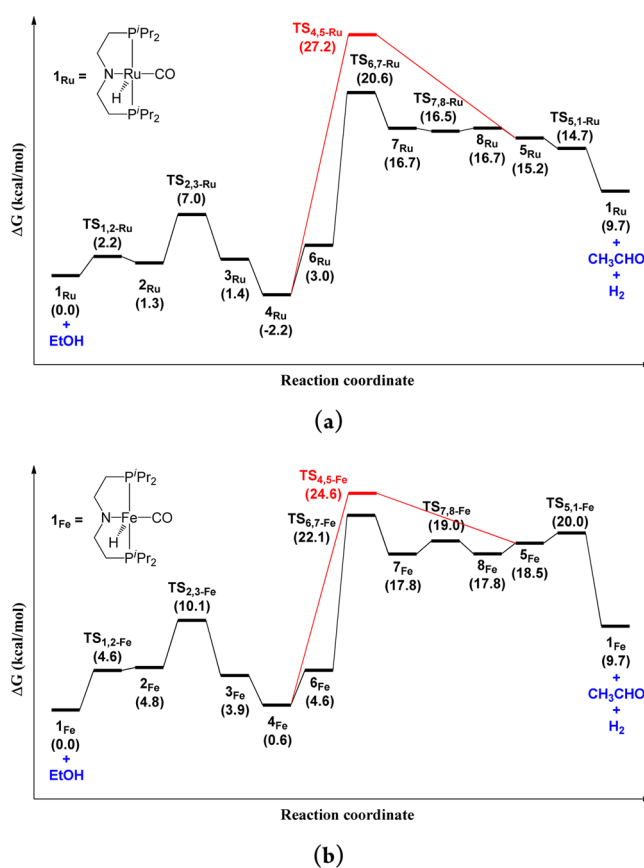
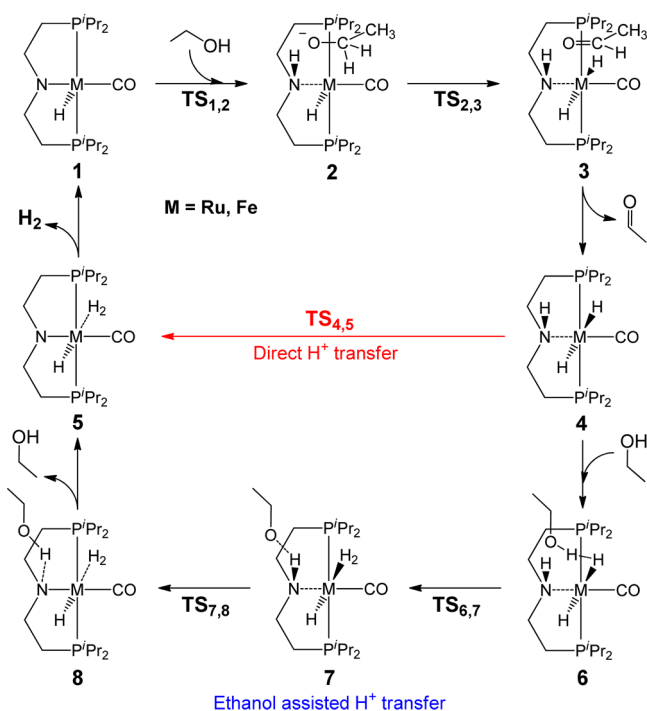


**Figure 1.** Free energy profile of the catalytic cycle shown in Scheme 1 for the experimental Ru catalyst (a) and its iron analogue (b) with ethanol-bridged proton transfer (black) and direct  $\text{H}_2$  formation (red) steps.

**Scheme 1. Catalytic Cycle for the Dehydrogenation of Ethanol with Direct Proton Transfer (Red) and Ethanol-Bridged Proton Transfer Pathways for the Formation of  $\text{H}_2$  and Acetaldehyde**



At the beginning of the reaction, an ethanol molecule approaches  $\mathbf{I}_{\text{Ru}}$  or  $\mathbf{I}_{\text{Fe}}$  and forms a slightly less stable intermediate  $\mathbf{2}_{\text{Ru}}$  or  $\mathbf{2}_{\text{Fe}}$ , respectively, through a quick transfer of the hydroxyl proton to the ligand nitrogen [TS<sub>1,2</sub> (Figure 2)]. The barrier for O–H bond cleavage is only 2.2 and 4.6 kcal/mol for Ru and Fe, respectively. Then a methylene hydride can easily transfer to the metal center through transition state TS<sub>2,3</sub> (Figure 2). An acetaldehyde molecule is therefore formed in  $\mathbf{3}_{\text{Ru}}$  or  $\mathbf{3}_{\text{Fe}}$ .  $\mathbf{3}_{\text{Ru}}$  or  $\mathbf{3}_{\text{Fe}}$  is very unstable. The dissociation of acetaldehyde from ( $\mathbf{3}_{\text{Ru}}$  and  $\mathbf{3}_{\text{Fe}}$ ) and the formation of a more stable *trans*-dihydride complex ( $\mathbf{4}_{\text{Ru}}$  and  $\mathbf{4}_{\text{Fe}}$ ) is a 3.6 and 3.3 kcal/mol downhill step for Ru and Fe, respectively.  $\mathbf{4}_{\text{Ru}}$  is 2.2 kcal/mol more stable than  $\mathbf{1}_{\text{Ru}}$ , but  $\mathbf{4}_{\text{Fe}}$  is 0.6 kcal/mol less stable than  $\mathbf{1}_{\text{Fe}}$ . Therefore,  $\mathbf{4}_{\text{Ru}}$  is the resting state in the observed dehydrogenation of ethanol catalyzed by aliphatic pincer Ru complexes.

To release  $\text{H}_2$  and regenerate the catalyst, the formation of a dihydrogen complex  $\mathbf{5}$  is required. If  $\mathbf{4}$  is the starting point, there are two pathways for the formation of  $\mathbf{5}$ . The more straightforward pathway is the direct transfer of a proton from the ligand nitrogen to the metal center through transition state TS<sub>4,5</sub> (Figure 2). However, calculation results indicate that the free energy barrier of this direct proton transfer pathway is 29.4 kcal/mol for the Ru catalyst ( $\mathbf{4}_{\text{Ru}} \rightarrow \text{TS}_{4,5-\text{Ru}}$ ), which is too high to account for the observed reaction rate under mild

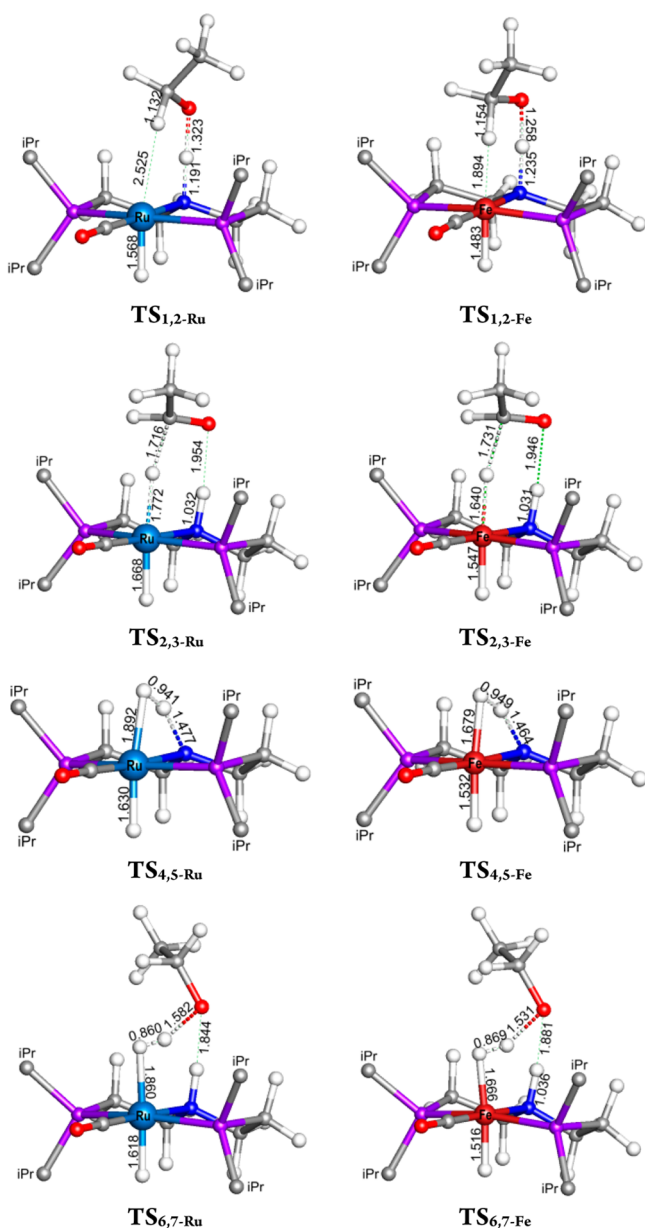


**Figure 2.** Optimized structures of key transition states  $TS_{1,2-Ru}$  ( $1227i\text{ cm}^{-1}$ ),  $TS_{1,2-Fe}$  ( $1084i\text{ cm}^{-1}$ ),  $TS_{2,3-Ru}$  ( $540i\text{ cm}^{-1}$ ),  $TS_{2,3-Fe}$  ( $470i\text{ cm}^{-1}$ ),  $TS_{4,5-Ru}$  ( $1163i\text{ cm}^{-1}$ ),  $TS_{4,5-Fe}$  ( $1150i\text{ cm}^{-1}$ ),  $TS_{6,7-Ru}$  ( $462i\text{ cm}^{-1}$ ), and  $TS_{6,7-Fe}$  ( $628i\text{ cm}^{-1}$ ). Isopropyl groups were omitted for the sake of clarity. Bond lengths are in angstroms.

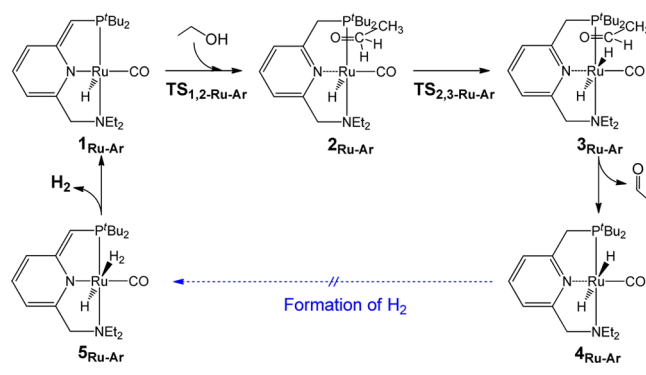
conditions. Interestingly, the calculated energy barrier of direct  $H_2$  formation in the iron complex ( $4_{Fe} \rightarrow TS_{4,5-Fe}$ ) is 5.4 kcal/mol lower than that of direct  $H_2$  formation in the Ru complex.

Instead of direct proton transfer, we found that an extra ethanol molecule can act as a proton transfer tunnel and assist the formation of  $H_2$ . In this self-promoted pathway, an ethanol molecule approaches **4** and forms a slightly less stable intermediate **6** with a strong intermolecular metal dihydrogen interaction. The  $H^{\delta-} \cdots H^{\delta+}$  distances are 1.657 and 1.620 Å in  $6_{Ru}$  and  $6_{Fe}$ , respectively. Such small  $H^{\delta-} \cdots H^{\delta+}$  distances are shorter than the  $H \cdots H$  distances in a range of 1.7–2.2 Å in most  $M-H^{\delta-} \cdots H^{\delta+}-X$  dihydrogen bonds reported so far.<sup>16</sup> Similar strong intermolecular  $Fe-H^{\delta-} \cdots H^{\delta+}-O$  dihydrogen bonds were reported in our recent theoretical studies.<sup>17</sup> After the formation of **6**, the hydroxyl proton in ethanol can transfer

to the metal hydride through transition state  $TS_{6,7}$  and forms a less stable intermediate **7**. The ethoxide group in **7** can easily take a proton from the ligand nitrogen and re-form an ethanol molecule through transition state  $TS_{7,8}$ . The dissociation of the re-formed ethanol molecule from  $8_{Ru}$  or  $8_{Fe}$  and the formation of  $5_{Ru}$  or  $5_{Fe}$  is a 1.5 kcal/mol downhill step for Ru or a 0.7 kcal/mol uphill step for Fe. The release of  $H_2$  from  $5_{Ru}$  for the regeneration of catalyst  $1_{Ru}$  is 5.5 kcal/mol downhill. The energy barrier for dissociation of  $H_2$  from  $5_{Fe}$  and the regeneration of  $1_{Fe}$  is only 1.5 kcal/mol. After comparing all relative energies shown in Figure 1, we can conclude that the simultaneous O–H bond cleavage and H–H bond formation process ( $TS_{6,7}$ ) is the rate-determining step in the whole catalytic reaction with total energy barriers of 22.8 and 22.1 kcal/mol for Ru ( $4_{Ru} \rightarrow TS_{6,7-Ru}$ ) and Fe ( $1_{Fe} \rightarrow TS_{6,7-Fe}$ ), respectively. The  $H_2$  formation barriers are decreased 6.6 and 2.5 kcal/mol by an extra ethanol molecule for Ru and Fe, respectively.

To explain the low catalytic activity of aromatic PNN pincer ruthenium complex  $1_{Ru-Ar}$  in the dehydrogenation of ethanol, we have calculated several key intermediates and transition states in a catalytic cycle. As shown in Scheme 2, the formation

### Scheme 2. Catalytic Cycle for the Dehydrogenation of Ethanol Catalyzed by $1_{Ru-Ar}$



of an aromatized *trans*-dihydride complex *trans*-(PNN)Ru( $H_2$ )CO ( $4_{Ru-Ar}$ ) and a dearomatized dihydrogen complex (PNN)Ru(H)CO( $H_2$ ) ( $5_{Ru-Ar}$ ) is required for the release of  $H_2$  from ethanol. Figure 3 shows calculated relative free energies of the structures in Scheme 2. Calculation results indicate that the aromatized *trans* dihydride complex *trans*-

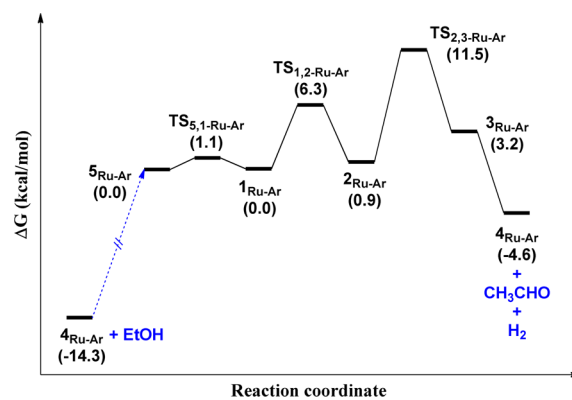


**Figure 3.** Relative free energies in the catalytic cycle shown in Scheme 2.



(PNN)Ru(H)<sub>2</sub>CO (**4**<sub>Ru-Ar</sub>) is 14.3 kcal/mol more stable than **1**<sub>Ru-Ar</sub>. Although the transition state (**TS**<sub>1,2-Ru-Ar</sub>) for the cleavage of the O–H bond in ethanol and the formation of aromatized intermediate **2**<sub>Ru-Ar</sub> is only 6.3 kcal/mol higher than **1**<sub>Ru-Ar</sub>, the transition state (**TS**<sub>2,3-Ru-Ar</sub>) for the cleavage of the methylene O–H bond in **2**<sub>Ru-Ar</sub> and the formation of acetaldehyde is 11.5 kcal/mol higher than **1**<sub>Ru-Ar</sub>. Therefore, the total free energy barrier of the dehydrogenation of ethanol catalyzed by **1**<sub>Ru-Ar</sub> is at least 25.8 kcal/mol (**4**<sub>Ru-Ar</sub> → **TS**<sub>2,3-Ru-Ar</sub>). Such a high energy barrier explains why the aromatic pincer ruthenium complex exhibited almost no catalytic activity for dehydrogenation of ethanol under mild conditions.

In summary, our computational study reveals that the dehydrogenation of ethanol catalyzed by aliphatic PNP pincer ruthenium complexes undergoes a self-promoted catalytic mechanism, which features an ethanol molecule acting as a proton transfer tunnel to lower the energy barrier for the formation of H<sub>2</sub>. The nitrogen atom in such a noninnocent aliphatic PNP ligand assists the cleavage and formation of the O–H bond in ethanol and plays a key role in the catalytic reaction. Furthermore, we have evaluated the potential of an iron analogue of **1**<sub>Ru</sub>, **1**<sub>Fe</sub>, as a catalyst for the dehydrogenation of ethanol. The calculated total free energy barrier of ethanol dehydrogenation catalyzed by **1**<sub>Fe</sub> is only 22.1 kcal/mol, which is even 0.7 kcal/mol lower than the calculated energy barrier of **1**<sub>Ru</sub>. Therefore, **1**<sub>Fe</sub> and its analogues have the potential to be developed as low-cost and high-efficiency catalysts for the production of hydrogen from alcohols.

## ■ ASSOCIATED CONTENT

### ● Supporting Information

Computational details, evaluation of the accuracy of the integration grid, calculated absolute free energies, and atomic coordinates of all optimized structures. This material is available free of charge via the Internet at <http://pubs.acs.org>.

## ■ AUTHOR INFORMATION

### Corresponding Author

\*E-mail: [xyang@iccas.ac.cn](mailto:xyang@iccas.ac.cn).

### Notes

The authors declare no competing financial interest.

## ■ ACKNOWLEDGMENTS

This work is supported by the 100-Talent Program of the Chinese Academy of Sciences (Y3290812R1) and the National Natural Science Foundation of China (21373228). Part of the computational work was performed in the Molecular Graphics and Computation Facility (MGCF) in the College of Chemistry of the University of California (Berkeley, CA). MGCF is supported by the U.S. National Science Foundation (CHE-0840505). I acknowledge the support of Dr. Kathleen A. Durkin.

## ■ REFERENCES

(1) Bockris, J. O'm. *Energy: The Solar-Hydrogen Alternative*; Halsted Press: New York, 1975.  
(2) (a) Subramani, V.; Song, C. *Catalysis* **2007**, *20*, 65–106. (b) Ni, M.; Leung, D. Y. C.; Leung, K. H. M. *Int. J. Hydrogen Energy* **2007**, *32*, 3238–3247. (c) Bion, N.; Duprez, D.; Epron, F. *ChemSusChem* **2012**, *5*, 76–84. (d) Navarro, R. M.; Sánchez-Sánchez, M. C.; Alvarez-Galvan, M. C.; Del Valle, F.; Fierro, J. L. G. *Energy Environ. Sci.* **2009**, *2*, 35–54. (e) Goldemberg, J. *Science* **2007**, *315*, 808–810. (f) Navarro,

R. M.; Peña, M. A.; Fierro, J. L. G. *Chem. Rev.* **2007**, *107*, 3952–3991. (g) Deluga, G. A.; Salge, J. R.; Schmidt, L. D.; Verykios, X. E. *Science* **2004**, *303*, 993–997. (h) Rostrup-Nielsen, J. R. *Science* **2005**, *308*, 1421. (i) Rodríguez-Lugo, R. E.; Trincado, M.; Vogt, M.; Tewes, F.; Santiso-Quinones, G.; Grützmacher, H. *Nat. Chem.* **2013**, *5*, 342–347. (j) Gunanathan, C.; Milstein, D. *Science* **2013**, *341*, 1229712. (k) Nielsen, M.; Alberico, E.; Baumann, W.; Drexler, H.-J.; Junge, H.; Gladiali, S.; Beller, M. *Nature* **2013**, *495*, 85–89. (l) Stephan, D. W. *Nature* **2013**, *495*, 54–55.

(3) (a) Johnson, T. C.; Morris, D. J.; Wills, R. *Chem. Soc. Rev.* **2010**, *39*, 81–88. (b) Junge, H.; Loges, B.; Beller, M. *Chem. Commun.* **2007**, 522–524. (c) Fujita, K.-I.; Tanino, N.; Yamaguchi, R. *Org. Lett.* **2007**, *9*, 109–111. (d) Fujita, K.-I.; Yoshida, T.; Imori, Y.; Yamaguchi, R. *Org. Lett.* **2011**, *13*, 2278–2281. (e) Dobereiner, G. E.; Crabtree, R. H. *Chem. Rev.* **2010**, *110*, 681–703. (f) Gnanaprakasam, B.; Zhang, J.; Milstein, D. *Angew. Chem., Int. Ed.* **2010**, *49*, 1468–1471. (g) Gunanathan, C.; Shimon, L. J. W.; Milstein, D. *J. Am. Chem. Soc.* **2009**, *131*, 3146–3147. (h) Zhang, J.; Leitus, G.; Ben-David, Y.; Milstein, D. *J. Am. Chem. Soc.* **2005**, *127*, 10840–10841. (i) Musa, S.; Shaposhnikov, I.; Cohen, S.; Gelman, D. *Angew. Chem., Int. Ed.* **2011**, *50*, 3533–3537. (j) Milstein, D. *Top. Catal.* **2010**, *53*, 915–923. (k) Gunanathan, C.; Ben-David, Y.; Milstein, D. *Science* **2007**, *317*, 790–792. (l) Shahane, S.; Fischmeister, C.; Bruneau, C. *Catal. Sci. Technol.* **2012**, *2*, 1425–1428.

(4) (a) Morton, D.; Cole-Hamilton, D. J. *Chem. Soc., Chem. Commun.* **1987**, 248–249. (b) Morton, D.; Cole-Hamilton, D. J. *Chem. Soc., Chem. Commun.* **1988**, 1154–1156. (c) Morton, D.; Cole-Hamilton, D. J.; Utuk, I. D.; Paneque-Sosa, M.; Lopez-Poveda, M. J. *Chem. Soc., Dalton Trans.* **1989**, 489–495.

(5) Nielsen, M.; Kammer, A.; Cozzula, D.; Junge, H.; Gladiali, S.; Beller, M. *Angew. Chem., Int. Ed.* **2011**, *50*, 9593–9597.

(6) Nielsen, M.; Junge, H.; Kammer, A.; Beller, M. *Angew. Chem., Int. Ed.* **2012**, *51*, 5711–5713.

(7) (a) Spasyuk, D.; Smith, S.; Gusev, D. G. *Angew. Chem., Int. Ed.* **2012**, *51*, 2772–2775. (b) Bertoli, M.; Choualeb, A.; Lough, A. J.; Moore, B.; Spasyuk, D.; Gusev, D. G. *Organometallics* **2011**, *30*, 3479–3482. (c) Spasyuk, D.; Gusev, D. G. *Organometallics* **2012**, *31*, 5239–5242.

(8) Bullock, R. M., Ed. *Catalysis Without Precious Metals*; Wiley-VCH: Weinheim, Germany, 2010.

(9) (a) Yang, X. *ACS Catal.* **2011**, *1*, 849–854. (b) Langer, R.; Diskin-Posner, Y.; Leitus, G.; Shimon, L. J. W.; Ben-David, Y.; Milstein, D. *Angew. Chem., Int. Ed.* **2011**, *50*, 9948–9952.

(10) (a) Langer, R.; Iron, M. A.; Konstantinovskii, L.; Diskin-Posner, Y.; Leitus, G.; Ben-David, Y.; Milstein, D. *Chem.—Eur. J.* **2012**, *18*, 7196–7209. (b) Langer, R.; Leitus, G.; Ben-David, Y.; Milstein, D. *Angew. Chem., Int. Ed.* **2011**, *50*, 2120–2124.

(11) Vasudevan, K. V.; Scott, B. L.; Hanson, S. K. *Eur. J. Inorg. Chem.* **2012**, *30*, 4898–4906.

(12) Frisch, M. J.; Trucks, G. W.; Schlegel, H. B.; Scuseria, G. E.; Robb, M. A.; Cheeseman, J. R.; Scalmani, G.; Barone, V.; Mennucci, B.; Petersson, G. A.; Nakatsuji, H.; Caricato, M.; Li, X.; Hratchian, H. P.; Izmaylov, A. F.; Bloino, J.; Zheng, G.; Sonnenberg, J. L.; Hada, M.; Ehara, M.; Toyota, K.; Fukuda, R.; Hasegawa, J.; Ishida, M.; Nakajima, T.; Honda, Y.; Kitao, O.; Nakai, H.; Vreven, T.; Montgomery, J. A., Jr.; Peralta, J. E.; Ogliaro, F.; Bearpark, M.; Heyd, J. J.; Brothers, E.; Kudin, K. N.; Staroverov, V. N.; Kobayashi, R.; Normand, J.; Raghavachari, K.; Rendell, A.; Burant, J. C.; Iyengar, S. S.; Tomasi, J.; Cossi, M.; Rega, N.; Millam, N. J.; Klene, M.; Knox, J. E.; Cross, J. B.; Bakken, V.; Adamo, C.; Jaramillo, J.; Gomperts, R.; Stratmann, R. E.; Yazyev, O.; Austin, A. J.; Cammi, R.; Pomelli, C.; Ochterski, J. W.; Martin, R. L.; Morokuma, K.; Zakrzewski, V. G.; Voth, G. A.; Salvador, P.; Dannenberg, J. J.; Dapprich, S.; Daniels, A. D.; Farkas, Ö.; Foresman, J. B.; Ortiz, J. V.; Cioslowski, J.; Fox, D. J. *Gaussian 09*, revision C.01; Gaussian, Inc.: Wallingford, CT, 2009.

(13) Zhao, Y.; Truhlar, D. G. *J. Chem. Phys.* **2006**, *125*, 194101.

(14) (a) Hehre, W. J.; Ditchfield, R.; Pople, J. A. *J. Chem. Phys.* **1972**, *56*, 2257–2261. (b) Hariharan, P. C.; Pople, J. A. *Theor. Chim. Acta*

1973, 28, 213–222. (c) Krishnan, R.; Binkley, J. S.; Seeger, R.; Pople, J. A. *J. Chem. Phys.* **1980**, 72, 650–654.

(15) Martin, J. M.; Sundermann, A. *J. Chem. Phys.* **2001**, 114, 3408–3420.

(16) Custelcean, R.; Jackson, J. E. *Chem. Rev.* **2001**, 101, 1963–1980.

(17) (a) Yang, X. *Dalton Trans.* **2013**, 42, 11987–11991. (b) Yang, X. *Inorg. Chem.* **2011**, 50, 12836–12843.